# Topological transformations in bipolar shells of nematic liquid crystals

T. Lopez-Leon and A. Fernandez-Nieves
*School of Physics, Georgia Institute of Technology, Atlanta, Georgia 30332, USA*
(Received 11 October 2008; published 26 February 2009)

We investigate how defects in bipolar shells of liquid crystal evolve when the boundary conditions for the nematic director $\boldsymbol{n}$ at the outer surface of the shell are changed from tangential to homeotropic. When the boundary conditions for $\boldsymbol{n}$ are tangential, these bipolar shells are characterized by the presence of two pairs of boojums, one pair on each spherical surface. However, when $\boldsymbol{n}$ is tangential at the inner surface and perpendicular at the outer surface, only the innermost pair of defects remains. Interestingly, there are two possible routes from one shell to the other and both involve the generation of a disclination ring that shrinks with time, eventually disappearing. Although the process is reminiscent of that encountered in bulk nematic droplets, in the case of nematic shells the two defects on the inner surface play a relevant role in the overall evolution process.

DOI: 10.1103/PhysRevE.79.021707 PACS number(s): 61.30.Jf, 47.55.D−

Nematic liquid crystal drops are technologically relevant since their optical properties can be electrically tuned; a fact that is exploited in simple and holographic polymer-dispersed liquid crystals [1–5]. In addition, nematic drops are fundamentally relevant since they often contain regions where the order parameter or director field $\boldsymbol{n}$, which gives the local orientational order of the system, is undefined. As a result, nematic drops often incorporate topological defects in their ground states; a fact that allows the study of defect interactions and defect transformations either when the boundary conditions for $\boldsymbol{n}$ at the confining surface are changed [6–8] or when external fields are applied [9–11].

Confinement of nematic liquid crystals inside spherical volumes imposes unavoidable topological constraints on $\boldsymbol{n}$, which often result in the presence of defects; these are characterized by their topological charge $s$, quantifying how much $\boldsymbol{n}$ rotates about the defect core. When the anchoring of $\boldsymbol{n}$ is tangential or parallel to the bounding surface, a theorem due to Poincaré and Hopf requires a total topological charge of $s=+2$ on the surface [12,13]. By contrast, when $\boldsymbol{n}$ is homeotropic or perpendicular to the surface, the total charge must be $s=+1$ and must be contained inside the spherical volume [14–16]; in this case, there are no defects on the surface. Albeit the restrictive character of these theorems, there are many possible nematic configurations inside the drops; these result from energy minimization. Indeed, the final drop configuration results from the minimization of the Frank-Oseen free energy density [17]:

$$f=\frac{1}{2}K_1(\mathrm{div}\,\vec{n})^2+\frac{1}{2}K_2(\vec{n}\cdot\mathrm{curl}\vec{n})^2+\frac{1}{2}K_3(\vec{n}\times\mathrm{curl}\vec{n})^2,$$

where $K_1$, $K_2$, and $K_3$ are the splay, twist, and bend elastic constants. The system is driven to a specific configuration that minimizes the free energy while complying with the topological constraints imposed by the boundaries.

Nematics with $K_1/K_3<1$ typically form bipolar drops, if $\boldsymbol{n}$ is tangential to the bounding surface, and radial drops, if the boundary conditions for $\boldsymbol{n}$ are perpendicular on this surface. Bipolar drops are characterized by two surface defects or boojums, which have topological charge $s=+1$ and are a droplet diameter away, as shown schematically in Fig. 1(a). Radial droplets, however, only contain a single point defect or hedgehog at the droplet center, as schematically shown in Fig. 1(e). Remarkably, the transformation from a bipolar to a radial configuration, which can be achieved by changing the nematic anchoring from parallel to perpendicular, involves intricate dynamics where new defects appear and evolve at the expense of the original defects of the bipolar drop [6,15]. The process proceeds via the transformation of the initial bipolar structure [Fig. 1(a)] into a transient, axial structure, which results from the perpendicular anchoring of the director and that is characterized by the presence of a closed defect line located along the drop equator, as schematically shown in Fig. 1(b). The symmetrical location of this defect ring with respect to the original location of the point defects in the bipolar drop results from the orientation of the nematic in the bulk of the drop, which does not change as the drop transforms from bipolar to axial; it remains oriented along the original boojum axis. Subsequently, the closed line shrinks [Fig. 1(c)] and disappears, leaving a point defect on the surface of the drop [Fig. 1(d)]. This defect then migrates toward the center; it is a hedgehog, which is a point defect in three dimensions, and characterizes the radial configuration shown in Fig. 1(e) [18].

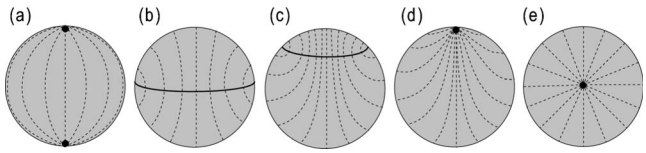


FIG. 1. Topological transformations undergone by a bipolar drop when the boundary conditions are changed from tangential to homeotropic. The schematics show a cross section of the drop along the plane containing the two initial boojums and the center of the sphere. The solid line refers to the defect line, which is always on the surface of the sphere, while the dotted lines refer to the director field inside the drop. In this process the bipolar drop (a) transforms into a transient axial drop (b), characterized by an equatorial disclination line. Subsequently, this line gradually shrinks (c) and eventually disappears leading to the formation of a point defect (d), which then migrates to the droplet center to form the final radial droplet (e). See [6,15] for further details.

 

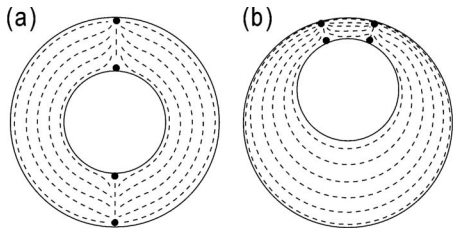


FIG. 2. (a) Bipolar shell with the two pairs of boojums aligned along the diameter of the largest bounding sphere. (b) Bipolar shell of inhomogeneous thickness. The shell is thinnest at the top, where the two pairs of defects are located.

Even more fascinating nematic structures should result when the nematic is confined to a spherical shell rather than to a drop. Indeed, for tangential boundary conditions on both surfaces, there are many possible structures which can differ in the number and type of defects, as well as on their location [19–24]. Among all of them, for sufficiently thick shells, a bipolar shell structure is theoretically expected [24]. In this case, there is an extra pair of $s=+1$ boojums in the additional inner surface of the shell, as schematically shown in Fig. 2(a). There is an extra boojum in the inner surface for each of the two defects in the outer surface; those on the inner surface are half hyperbolic hedgehogs and can be distinguished in this sense from those on the outer surface, which are half radial hedgehogs [25].

Recent experiments with nematic shells have revealed the existence of bipolar shells [19]. However, in this case, the pairs of surface defects are not located along a diameter of the larger sphere but instead are located at the top of the shell, as schematically shown in Fig. 2(b); this results from the inhomogeneous thickness of these shells, which are thinnest at the top, precisely where the defects are found. The equilibrium distance between defects is determined by the balance between the elastic distortions in the bulk of the shell and the repulsion between defects with the same topological charge, as recently confirmed by computer simulations [20].

By contrast to these bipolar shells, when the anchoring is perpendicular on both surfaces, no defects are required anywhere inside the shell; the presence of the inner sphere provides the $s=+1$ defect required by the Gauss theorem [26]. The change in the boundary conditions for $\boldsymbol{n}$ dramatically changes the nematic structure and the resultant defect configuration. By contrast to nematic drops, in this case, there are two spherical surfaces whose boundary conditions can be independently tuned. Despite this fact, there are neither experimental observations nor theoretical predictions for the defect evolution when the nematic anchoring at either bounding surface changes from tangential to homeotropic.

In this paper, we investigate how the defect structure of a bipolar shell evolves after the boundary conditions in the outer surface are changed from parallel to perpendicular. We find that the route toward the final equilibrium configuration involves the generation, disappearance, and transformation of the original defects. In analogy to nematic drops, a transient closed disclination line forms. However, for shells, we find two distinct pathways to the final equilibrium state,

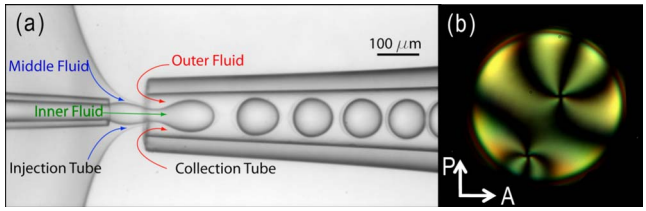


FIG. 3. (Color online) (a) Microcapillary device employed for generating double emulsions. (b) Cross-polarized image of a typical bipolar shell of nematic liquid crystal generated with this microcapillary device. $R=25$ $\mu$m and $R-a=1$ $\mu$m.

which incorporates two boojums on the inner surface and no defects in the outer surface. Irrespective of the route, at the end of the process, the disclination ring always encircles one of the two inner defects, causing a change in its character right after the line disappears; it changes from a half hyperbolic to a half radial hedgehog.

To make spherical shells of nematic liquid crystal we generate double emulsions using an axisymmetric microfluidic device that produces a coaxial flow which is hydrodynamically focused by the outermost fluid through a narrow orifice of the collection tube [27], as shown by the optical micrograph in Fig. 3(a). The outer fluid of the coaxial flow is a nematic liquid crystal, pentyl-cyano-biphenyl (5CB). The innermost and outermost fluids are water containing 1 wt % of poly(vinyl alcohol) (PVA) which ensures stability of the double emulsion and ultimately enforces tangential boundary conditions for the nematic liquid crystal [4,28]. The resultant double emulsion drops consist of an inner water drop, of radius $a$, and a shell of liquid crystal, all immersed in water. The overall radius of the compound drop is $R$.

Using this method we can generate bipolar shells, like that shown in the cross-polarized image of Fig. 3(b). The observed texture results from a nematic arrangement inside the shell that approximately corresponds to the schematic shown in Fig. 2(b). In our shells, the density difference between 5CB and the inner drop, $\rho_{5CB}-\rho_{water}$ (293 K)$=26.7$ kg/m$^3$ [29], causes a local thinning of the shell at its top. As a consequence, our shells are heterogeneous in thickness; this results in the location of the defects at the uppermost part of the shell. The defects are characterized by four black brushes, indicative of a topological charge of $s=+1$. However, because of the small thickness of the shell at its top, we can only observe the defect pair on the outer drop; there must be a second pair approximately below this one, as required by the Poincaré theorem.

We change the surface anchoring on the outer drop by adding a concentrated solution of sodium docecyl sulphate (SDS) to the continuous phase after the double emulsions are collected on a microscope glass slide. This surfactant is known to induce perpendicular anchoring of the nematic [30], thus leading to the formation of a hybrid bipolar shell. Although PVA is not removed from the medium, the high concentration of SDS employed, typically four times its critical micelle concentration, guarantees that the homeotropic alignment of the molecules has been achieved. This process is not instantaneous since the SDS molecules need certain time to diffuse to the shell. However, eventually a closed

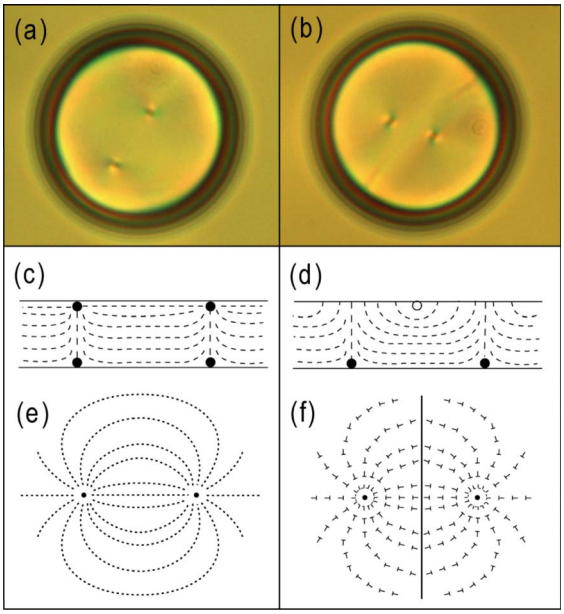


FIG. 4. (Color online) (a), (b) Bright field micrographs of the shell just before and after the line is formed. (c), (e) When the boundary conditions are tangential at both surfaces, the defect structure is characterized by two pairs of half hedgehogs in either surface, as shown in (c), which corresponds to a side view of the shell; (e) represents the nematic orientation, as seen from above the shell. (d), (f) After changing the anchoring at the outer surface of the shell from tangential to homeotropic, the two boojums on the outer surface disappear and a disclination line, represented by the hollow circle, forms; this line surrounds the shell. In (f) we schematically show the projection of $\boldsymbol{n}$ onto the outer surface, where the heads of the nails indicate an upward tilt of $\boldsymbol{n}$ as we move from the inner to the outer surface. In this representation, it is clear that the line induces a $\pi$ jump in this projected director field.

defect line forms, setting the start of the process. This line appears on the outer surface, on the middle plane between the axis joining the original two defects, as shown in the bright field images of Figs. 4(a) and 4(b), which correspond to the top of the shell just before and after the line is formed. The origin of this defect line is similar to that of the equatorial line arising in the transformation from bipolar to radial drops. It thus results from the combination of perpendicular anchoring on the outer surface with the existing bipolar director field in the bulk of the shell.

Before the formation of the line, there are two boojums on the outer surface, as shown schematically in Fig. 4(c), which corresponds to a cross section of the top of the shell in this situation, and in Fig. 4(e), which shows the corresponding top view. After the anchoring changes to homeotropic, these defects disappear causing the unavoidable delocalization of the director in the region between the original two point defects, as shown schematically in Fig. 4(d), which corresponds to a cross section of the top of the shell in this new situation, and in Fig. 4(f), which shows the corresponding top view. In the side view of the shell [Fig. 4(d)], the disclination line is shown as a hollow circle, while in the top view of the shell [Fig. 4(f)], we use nails to represent the projection of the director field onto the outer surface of the shell. In this case, we see that the disclination line arises from the $\pi$ jump in this projected field.

Once the disclination ring is formed, the boojums on the inner surface move away from each other along the direction of the line, as shown in Figs. 5(a) and 6(a), which are two representative cross-polarized images of the initial evolution of the point defects after formation of the line, and in the corresponding schematics below the images. Subsequently, the line shrinks and eventually disappears. Surprisingly, however, there are two different pathways for this process. In the first one, the boojums separate from the line and align along the normal to the plane containing the disclination ring, as shown for the upper boojum in the bright field image of Fig. 5(b) and in the corresponding schematic below the image; this occurs ~12 min from the formation of the line and corresponds to a boojum-boojum separation of around an inner-drop diameter. The rest of the process involves the shrinkage of the line around one of the two defects, as shown in Figs. 5(c)–5(e) and in the corresponding schematics below the images. We emphasize, however, that the line lies on the outer surface, while the defects are located on the inner surface.

The second scenario is qualitatively different. In this case, the boojums are also located below the defect line, but on opposite sides of the ring, as shown in Figs. 6(b)–6(d) and in

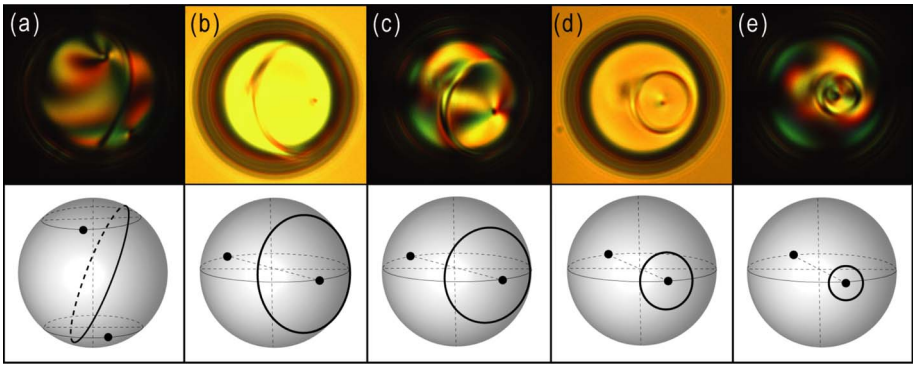


FIG. 5. (Color online) Shrinkage of the disclination ring around one of the inner-surface boojums. (b) and (d) are images taken in bright field, while (a), (c), and (e) are taken between crossed polarizers. The schematics below show the approximate position of the point defects with respect to the disclination line. The lapse time since the generation of the line is (a) 0, (b) 12, (c) 20, (d) 25, and (e) 30 min. $R=23$ $\mu$m and $R-a=2$ $\mu$m.

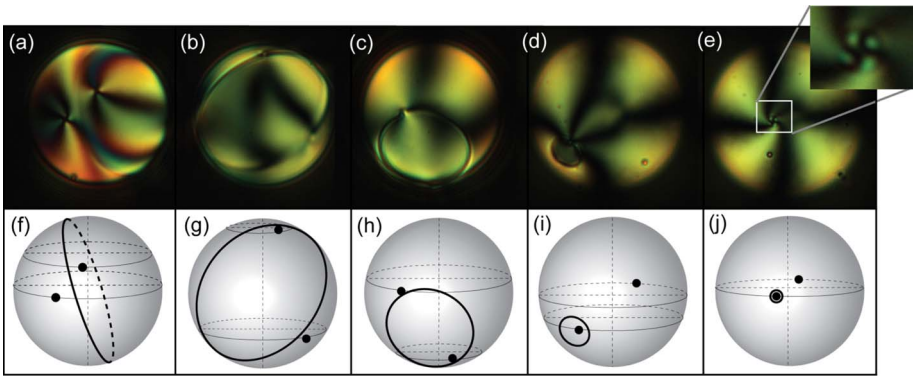


FIG. 6. (Color online) Cross-polarized images corresponding to the shrinkage of the disclination ring in the second scenario. In this case, the defects remain below the line separated by approximately a ring diameter The schematics below show the approximate position of the point defects with respect to the disclination line. The lapse time since the generation of the line is (a) 0, (b) 4, (c) 19, (d) 29, and (e) 33 min. In (e), the two boojums have migrated away; one of them relocates below the center of the small disclination ring, while the other is an inner-drop diameter away. $R=35$ $\mu$m and $R-a=3$ $\mu$m.

the corresponding schematics below the images. However, as the ring gets smaller, the repulsion between point defects increases, eventually becoming high enough to induce their rapid separation. At this point, the boojums migrate and become separated by an inner-drop diameter, as shown in Fig. 6(e) and in the corresponding inset, where both the defect and the ring are visible; this occurs ~30 min after formation of the closed disclination line.

We observe both routes irrespective of the shell thickness and overall size, which we varied between $R-a=1$ $\mu$m and 10 $\mu$m, for $R$ within 20 and 90 $\mu$m. However, the first route [Figs. 5(a)–5(e)] is more frequent for thicker shells, while the second route [Figs. 6(a)–6(e)] is more common for thinner shells. Since in thicker shells the inner drop is much smaller than the outer drop, the boojums on the inner surface interact with each other earlier in the defect evolution process; this favors their separation, causing their alignment with the center of the disclination ring. Consistent with this, the time scale associated to this defect migration is substantially different among both routes, as shown in Figs. 5(b) and 6(e), even though their overall time is not very different.

Both processes end with the final disappearance of the line and formation of the hybrid nematic shell. This new structure has no defects on the outer surface and has two defects on the inner one, as shown in Fig. 7; there is one defect at approximately the top of the shell [Fig. 7(a)] and one defect at approximately the bottom of the shell [Fig. 7(b)], both on the inner surface. Interestingly, these two defects can no longer both be half hyperbolic hedgehogs; otherwise the perpendicular and tangential boundary conditions for $\boldsymbol{n}$ at the bounding surfaces cannot be commensurate. Instead, one of the boojums must become a half radial hedgehog, as schematically shown in Fig. 8(a). This qualitative structural change in the vicinity of one of the two surface defects can be understood by looking at the final stages of the line shrinkage process, which we schematically show in Figs. 8(b) and 8(c). By identifying the director field orientation outside the defect line, one can readily observe that the line disappearance is accompanied by a change in the nature of the defect lying below the line, which changes from a half hyperbolic hedgehog to a half radial hedgehog. Therefore, the final collapse of the defect line also implies a configurational change of $\boldsymbol{n}$ around the defect it encircles in the final stages of the process.

We conclude that the transition from bipolar to hybrid bipolar shells induced by changing the anchoring of $\boldsymbol{n}$ at the outer surface involves the generation of a disclination ring, reminiscent of the transformation process from bipolar to radial drops. However, for shells, the subsequent evolution of this line can proceed via two different routes. For thinner shells, we typically see that the two defects on the inner surface remain below the ring at around a ring diameter away, while for thicker shells we typically see that one of these two defects remains below the center of the disclina-

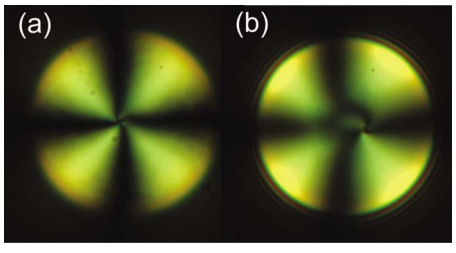


FIG. 7. (Color online) Cross-polarized images of a hybrid bipolar shell. (a) Upper and (b) lower defects.

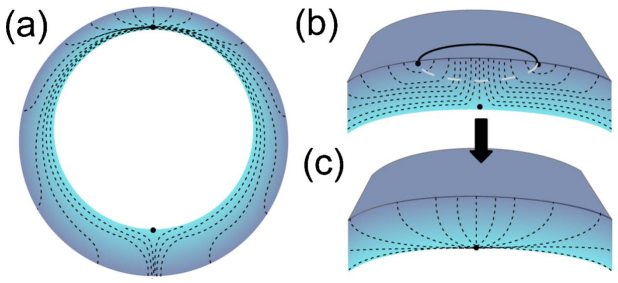


FIG. 8. (Color online) (a) Cross section of a hybrid bipolar shell with a half hyperbolic and a half radial hedgehog. (b), (c) Final evolution of the disclination ring emphasizing the required change in the nature of the defect below the line; it must change from a half hyperbolic (b) to a half radial hedgehog (c).

tion ring. We believe that the repulsion between defects can qualitatively account for these different pathways, although detailed nematohydrodynamic calculations are needed in order to support this interpretation. Finally, irrespective of the particular process, one of the defects in the inner surface must change from a half hyperbolic hedgehog to a half radial hedgehog; this naturally results from the disappearance of the disclination ring around one of the two boojums and is the only way to commensurate the imposed perpendicular boundary conditions on the outer surface of the shell with the imposed tangential boundary conditions on its inner surface.

We thank Professor David A. Weitz for his support. We also acknowledge Grant No. DPI2008-06624-C03-03.

[1] C. Paquet and E. Kumacheva, Mater. Today **11**, 48 (2008).
[2] T. J. Bunning, L. V. Natarajan, V. P. Tondiglia, and R. L. Sutherland, Annu. Rev. Mater. Sci. **30**, 83 (2000).
[3] L. Bouteiller and P. LeBarny, Liq. Cryst. **21**, 157 (1996).
[4] P. S. Drzaic, *Liquid Crystal Dispersions* (World Scientific, Singapore, 1995).
[5] S. J. Woltman, J. N. Eakin, G. P. Crawford, and S. Žumer, Opt. Lett. **31**, 3273 (2006).
[6] G. E. Volovik and O. D. Lavrentovich, Sov. Phys. JETP **58**, 1159 (1983).
[7] O. O. Prischepa, A. V. Shabanov, and V. Ya. Zyryanov, JETP Lett. **79**, 257 (2004).
[8] O. O. Prishchepa, A. V. Shabanov, and V. Ya. Zyryanov, Phys. Rev. E **72**, 031712 (2005).
[9] V. G. Bodnar, O. D. Lavrentovich, and V. M. Pergamenshchik, Sov. Phys. JETP **74**, 60 (1992).
[10] F. Xu, H. S. Kitzerow, and P. P. Crooker, Phys. Rev. E **49**, 3061 (1994).
[11] A. Fernandez-Nieves, D. R. Link, M. Marquez, and D. A. Weitz, Phys. Rev. Lett. **98**, 087801 (2007).
[12] H. Poincare, J. Math. Pures Appl. **1**, 167 (1885); H. Hopf, Math. Ann. **96**, 427 (1926).
[13] R. D. Kamien, Rev. Mod. Phys. **74**, 953 (2002).
[14] D. L. Stein, Phys. Rev. A **19**, 1708 (1979).
[15] O. D. Lavrentovich, Liq. Cryst. **24**, 117 (1998).
[16] M. Kleman and O. D. Lavrentovich, *Soft Matter Physics: An Introduction* (Springer, Berlin, 2003).
[17] P. G. De Gennes and J. Prost, *The Physics of Liquid Crystals* (Oxford University Press, Oxford, 1995).
[18] There is an alternative mechanism [7,8], where transition between bipolar and radial droplets occurs without the formation of additional defects. In this case, the boojums simply disappear as the final surface defect shown in Fig. 1(d) forms. This defect then migrates to the center of the drop, which becomes a radial drop.
[19] A. F. Fernandez-Nieves, V. Vitelli, A. S. Utada, D. R. Link, M. Marquez, D. R. Nelson, and D. A. Weitz, Phys. Rev. Lett. **99**, 157801 (2007).
[20] G. Skačej and C. Zannoni, Phys. Rev. Lett. **100**, 197802 (2008).
[21] H. Shin, M. J. Bowick, and X. Xing, Phys. Rev. Lett. **101**, 037802 (2008).
[22] J. Dzubiella, M. Schmidt, and H. Löwen, Phys. Rev. E **62**, 5081 (2000).
[23] M. A. Bates, J. Chem. Phys. **128**, 104707 (2008).
[24] V. Vitelli and D. R. Nelson, Phys. Rev. E **74**, 021711 (2006).
[25] The opposite situation in which the two half hyperbolic hedgehogs are on the inner surface and the two half radial hedgehogs are on the outer surface is also topologically possible.
[26] P. Poulin, H. Stark, T. C. Lubensky, and D. A. Weitz, Science **275**, 1770 (1997).
[27] A. S. Utada, E. Lorenceau, D. R. Link, P. D. Kaplan, H. A. Stone, and D. A. Weitz, Science **308**, 537 (2005).
[28] A. A. Sonin, *The Surface Physics of Liquid Crystals* (Gordon and Breach, London, 1995).
[29] J. Deschamps, J. P. M. Trusler, and G. Jackson, J. Phys. Chem. B **112**, 3918 (2008).
[30] Concentrations of SDS above 1*M* provide strong perpendicular anchoring of 5CB [31]. In our experiments the bulk concentration of SDS is always ~30 m*M*. We expect that the small concentration of PVA molecules, which is also present in the continuous phase after the boundary conditions are changed, does not significantly alter the homeotropic anchoring induced by the SDS since the number of PVA molecules is much smaller than those of SDS.
[31] J. M. Brake and N. L. Abbott, Langmuir **18**, 6101 (2002).